MECHANICAL PROPERTIES OF HYPOEUTECTIC, EUTECTIC, AND HYPEREUTECTIC AL-SI AUTOMOTIVE ALLOYS UNDER AGEING TREATMENT

Dewan Salsabil Ahammed[1] – Ahmed Asif Razin[1] – Akib Abdullah Khan[1] – Mohammad Salim Kaiser[2*]

[1]Department Mechanical Engineering, Bangladesh University of Engineering and Technology, Dhaka-1000, Bangladesh
[2]Innovation Centre, International University of Business Agriculture and Technology, Dhaka-1230, Bangladesh

ARTICLE INFO

***Article history*:**
Received: 10.11.2022.
Received in revised form: 27.02.2023.
Accepted: 08.12.2023.

Keywords:
Al-Si-Cu-Mg alloys
Heat treatment
Tensile
Impact
Fractography

DOI: https://doi.org/10.30765/er.2063

Abstract:

The role of different levels of silicon on mechanical properties has been investigated through tensile and impact tests along with fractography of Al-Si automotive alloys. Cast alloys are given precipitation strengthening through T6 heat treatment. It has been experimentally determined that ageing these alloys leads to the enhancement of tensile properties, which is mainly caused by the precipitation of the intermetallics such as Al_2Cu, Mg_2Si, and Al_2CuMg within the Al-matrix. The ductility of these alloys primarily exhibit a diminishing trend as the ageing temperature increased. This diminishing trend can be attributed to the formation of fine precipitates like GP zones and metastable phases. However, after reaching a certain temperature, the ductility started to increase again. This is caused by the coarsening of the precipitates. At higher strain rates, the tensile strength is found to be identical for higher Si-added alloys due to their brittleness. The microstructures of the alloys reveal that as Si content increases, eutectic phases become more apparent. Fractography of the base alloy exhibits a small dimple structure, and higher Si-added alloys initiate the crack propagation. Beyond eutectic composition, the mechanical properties of the alloys became distorted due to block-like primary Si into the Al-matrix.

1 Introduction

When silicon is alloyed with aluminium, it is designated as a 4xxx series alloy. Due to its excellent castability, it is mainly used for manufacturing complex and high-strength automotive parts. This type of alloy has no unique mechanical properties because the significant element Si in the binary alloy does not form any intermetallics [1, 2]. To enhance the different properties, minor elements such as Mg, Zn, Cu, Ni, Sn, and Pb are added to the aluminium-silicon alloy to form a solid solution and enhance the solid solution strengthening [3-6]. The trace elements, namely Zr, Ti, Sc, Ce, etc., are added to this alloy to improve its properties through grain refinement. Some studies have demonstrated that impurities created during the casting of an alloy can improve the properties of the alloy [7, 8]. During casting, the impurities like Fe, Pb, and Mn can come from the melting environment.

These impurities appear from sources such as furnaces' refractory linings, ladles, reactors etc. Currently, reducing vehicle mass and production costs are of major concern in the automotive sector, as well as keeping safety and comfort intact. Using Al-Si alloys instead of cast iron in advanced engine components such as pistons and engine blocks, the mass can be reduced by about 50%. [9]. Among the various types of Al alloys, Al-Si-Cu-Mg alloys are significantly more used in different engineering sectors due to their various types of applications. In this type of alloy, the primary alloying element is silicon, and the high strength-to-weight ratio is one of their most attractive characteristics [10, 11]. As the properties are so adaptable, these alloys are extensively used in the automobile and aircraft industries at present times. Some of their recent uses include

* Corresponding author
E-mail address:dkaiser.res@iubat.edu

castings different cylinder components such as blocks, pistons for engines and crankcases etc. Three types of Al-Si automotive alloys can be classified based on the concentration of Si. When the Si content is 12.6wt% Si, the alloy is eutectic Al-Si alloy. Alloys containing lower and higher levels of Si are hypoeutectic and hypereutectic alloys, respectively [12]. Usually, hypoeutectic alloys are used for the lower strength sector and eutectic alloys for the moderate strength applications, while hypereutectic Al-Si alloys are considered for of heavy engine construction.

The addition of Cu and Mg during this heat treatment procedure can cause the formation of the Al_2Cu and Mg_2Si intermetallic hardening phases, which precipitate into the matrix of the alloys and strengthen these types of Al-Si alloys. Typically, T6 heat treatment includes solution treatment as it is performed at a temperature of about 530°C followed by aging beyond at a temperature of 175°C, with the aim of achieving precipitation hardness through various intermetallics. Many researchers have looked at the effects of applying a similar heat treatment, which they refer "type T6" [13-15]. To enhance the properties, around 2 wt.% of Cu and Mg of 0.5-1.0 wt.% has been added to this alloy. To get an idea about its properties, much work has been done on the Al-Si automotive alloys where different elements are considered, the amount of the elements is varied, and different process parameters also have been employed [16-18]. From the results, it can be said that all the aforementioned variance impacts the properties of the Al-Si automotive alloys. In the case of the primary alloying material, it improves one or more properties significantly and affects the other properties also. Furthermore, the quantity of the alloying elements plays a vital role in varying the alloy's properties [19, 20].

This work is undertaken to study the consequences of heat treatment on the mechanical properties of hypoeutectic, eutectic, and hypereutectic Al-Si automotive alloys. To isolate the effect of Si, only the Si content has been varied while the other elements of the alloy, like Cu, Mg and Fe, have been kept constant. A conventional casting process is used for this purpose. In addition, no and low amounts of Si have also been considered for a better understanding of the effect on the properties associated with tensile, impact, fracture, and microstructural behaviour of the alloys.

2 Experimental details

Commercial aluminium of 99.750 wt%, copper of 99.997 wt%, magnesium of 99.800 wt% purity and master alloy of Al-50 wt.% Si were used to develop the experimental hypoeutectic, eutectic, and hypereutectic Al-Si automotive alloys. Two extra alloys without Si as a base alloy and a minor concentration of Si have also been considered for clarification of the effect of Si variation on properties. During the preparation for the experiment, every element was weighed to the exact ratio requirement while also considering the additional amount for melting loss. The alloys used in this experiment were melted in a crucible of clay-graphite via a natural gas-fired pit furnace. Borax was also used as a degasser at some stage in melting. The furnace temperature was maintained at 750 ± 10 °C. Previous to casting, the molten metal in the crucible was homogenized by stirring at 700 °C. The temperature was monitored with the help of a non-contact digital laser temperature gun. Casting was accomplished in a mild steel mould, preheated at 250 °C, of 20 ×200 × 300 millimetres. The experimental alloy's chemical composition, shown in Table 1, was evaluated through an optical emission spectrometer, model Shimadzu PDA 700. Five samples of each alloy are considered and the average value of chemical composition is determined.

Table 1. Average elements composition by wt% from OES analysis of the experimental alloys.

	Si	Cu	Mg	Fe	Ni	Pb	Zn	Mn	Ti	Al
Alloy 1	0.244	2.158	0.767	0.211	0.199	0.163	0.076	0.065	0.005	Bal
Alloy 2	3.539	2.309	0.784	0.273	0.217	0.166	0.083	0.067	0.010	Bal
Alloy 3	6.149	2.113	0.754	0.301	0.264	0.163	0.111	0.073	0.012	Bal
Alloy 4	12.656	2.130	0.770	0.311	0.277	0.169	0.168	0.081	0.014	Bal
Alloy 5	17.851	2.190	0.755	0.321	0.281	0.167	0.198	0.097	0.021	Bal

The surfaces of the cast alloys were primarily machined for the removal of the oxide layer. During T6 heat treatment, initially, the machined alloys were allowed to homogenize at 450 °C for 12 hours; so that the precipitating elements become more evenly distributed throughout the material and air-cooled to relieve the

internal stresses. Solutionizing of the homogenized samples was carried out at a temperature of 535 °C for a duration of 2 hours which was then followed by quenching in salt ice water to get a single-phase supersaturated region. The tensile testing was performed in an Instron tensile testing machine at room temperature using different crosshead speeds to keep up the 10^{-4}/s, 10^{-3}/s, 10^{-2}/s and 10^{-1}/s strain rates. The samples used were machined according to ASTM specifications. The sample gauge length for the tensile test was 25 mm. For impact testing, samples of standard size of 10 ×10 × 55 mm, having a V-shaped notch of 2 mm deep and 45° angle, were used. Testing was performed according to ASTM E23. The solutionized samples were aged isochronally for one hour up to 350 °C at different temperatures. For this purpose, an electric muffle furnace JSMF-30T ranging from 900 ± 3.0 ºC was used. The tensile along with impact strength was determined by the average of five tests each. Specimens of the heat-treated alloys were subjected to optical metallographic studies and carried out in a standard manner.

The specimens were polished with sandpaper and finally with alumina, followed by being etched with Keller's reagent. The washed and dried samples were observed carefully in the Versamet-II microscope, and a number of chosen photomicrographs were taken. Fractured surfaces created by tensile testing were also observed by a Jeol scanning electron microscope type of JSM-5200.

3 Results and discussion

3.1 Tensile properties

The ultimate tensile strength of different Si-added Al-based automotive alloys was measured at the strain rate of 10^{-3}/s. Variation of these strengths under different isochronal ageing conditions for one hour is graphically presented in Figure 1. The figure demonstrates the significant changes in the tensile strength along with the increment of ageing temperature. It can be observed that the strength of all the alloys initially increased with an increase in temperature, followed by another rapidly increased and to end with a sharp decrease in strength as the ageing temperature is increased further. At the first stage of this ageing treatment around 100 °C, strengthening occurs due to the homogeneously distributed profuse and delicate GP zones in the matrix [21]. Secondly, in ageing at the intermediate stage, the metastable phases are formed and maintained with the matrix semi-coherence, which is more significant at the later stage.

The increase in tensile strength at GP zones and metastable phase formation can be explained by dislocation theory. The formed precipitates resist dislocation movement, which in turn increases tensile strength. However, these GP zones dissolve significantly as the ageing temperature increases and the formation of the metastable phase occurs. At this stage of dissolution, these metastable phases do not resist dislocation movement leading to lower strengthening effects [22]. Due to heat treatment and formation of the GP zones and metastable phase, the base Alloy 1 produces the intermetallic phases of Al_2Cu and Al_2CuMg, which improve the strength of the alloy [23]. When the Si-added alloys go through the heat treatment process, the additional intermetallic phases, like Mg_2Si, and Q-$Al_5Cu_2Mg_8Si_6$, are formed, and these intermetallics improve the strength [24]. Especially, Mg_2Si particles refine the α-Al grains and improve the interfacial link between reinforced Mg_2Si particles and the matrix. A higher fraction of these precipitates leads to a higher strength as the other elements in these alloys are constant [25]. Beyond the eutectic composition, 17.9Si alloy loses its strength because the excess Si stays slackly into the alloy's matrix [26].

Another observable fact from the Figure is that all the Si added alloys except the base alloy showed earlier ageing peaks with different intensities. From this experimental result, it can be said that the shifting of these peaks of strength is caused by the addition of Si into the automotive alloys. The GP zones, metastable phases etc. form earlier because of the following two reasons. It is well recognized that attractive binding forces exists between Si atoms and vacancies, so the formation of the Si-vacancy clusters performs as heterogeneous nucleation sites for the precipitates. A different possible explanation is the enhancement of the precipitate number density. It is caused by a reduction of the solubility of other elements due to the presence of Si in the matrix, which increases the chemical driving force for precipitation and decreases the reversible work for nucleation [27, 28]. Ageing at higher temperatures leads to a decrease in the strength of the alloys. This is due to precipitation and grain coarsening and recrystallization, which are also known as over-ageing. These coarse particles reduce the pinning effect, and dislocation movements happen more easily, resulting in lower tensile strength [29].

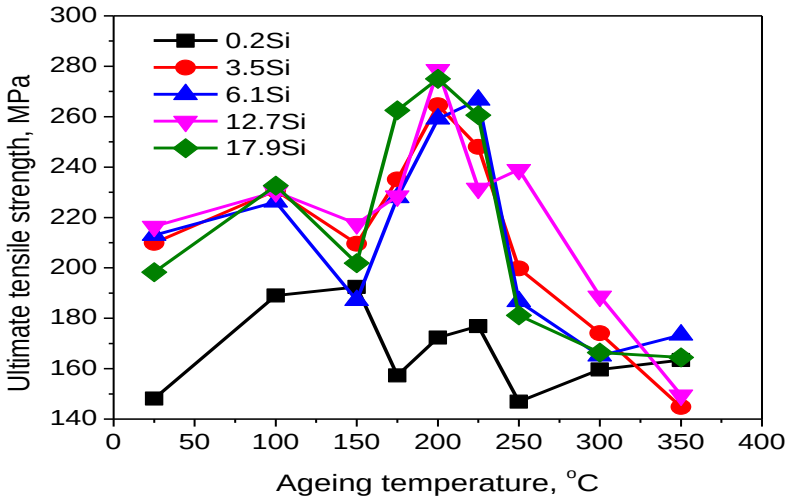

Figure 1. Ultimate tensile strength evolution for different Si added alloys during isochronally ageing for 1h.

Figure 2 provides the average values of the elongation percentages for all the alloys under different isochronal ageing conditions. The results demonstrate a scattered value throughout the ageing process that is sometimes higher and sometimes lower. It is very much known that throughout the ageing process this type of Al-Si-Cu-Mg alloy forms different phases like a supersaturated solid solution, GP zones, intermediate β″, intermetallic β′, equilibrium β and the Q″ phase [30]. These precipitation sequences are reflected in the form of ductility minima. Fine precipitates act as the early nucleation sites for microvoids. This leads to a decrease in the fracture resistance behaviour of the material. Total elongation is also reduced by the pinning effect of precipitated particles. The initial drop in elongation percentage is linked with the GP zone formation, which is followed by another drop due to the formation of metastable phases. Another thing to note is that the formation of an intermetallic apparently dissolves the previous one, at these stages of ageing, the opposite phenomenon of maximum ductility is observed. Finally the radical increase of energy occurs due to particle coarsening effects. These coarser particles markedly diminish the pinning effect allowing dislocations to move more easily than before [31].

One thing that can be noticed is that a tiny quantity of Si increases the elongation of the alloys. It refines the α-Al grains and improves the interfacial bonding between the reinforced Mg_2Si particles and matrix. At the peak aged condition, these properties go down because the maximum different fine precipitates isolate these properties. When the amount becomes higher, there is a propensity to create needle-like eutectic Si. Beyond the eutectic composition, the appearance of star-shaped blocky primary Si results in lower elongation [32]. It is well known that Si-rich intermetallics are incredibly brittle and rigid compounds. They act as stress raisers and the points of weakness in the alloy matrix. Consequently, the strength and ductility of the alloys reduce due to the micro-cracks formed due to these weak points in the matrix. The intermetallics also exist as separate particles with a highly faceted and relatively low bonding strength with the matrix, which is the cause of the degradation of ductility.

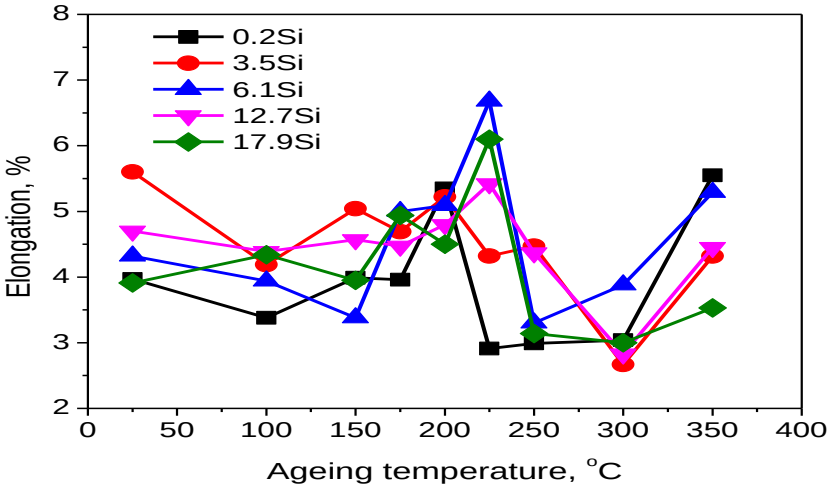

Figure 2. Percent elongation evolution for different Si added alloys during isochronally ageing for 1h.

The experimental results of the ultimate tensile strength tested under different strain rate are plotted in Figure 3. The tensile strength has been taken at the alloys peak aged condition that is solution treated at 535 °C for time of 2h and aged at 200 °C for 1h. It is clear from the Figure that the tensile strength is affected by the variation of strain rate, and the range of variation is short in the alloys with added Si. The improvement in strength could be due to the following two reasons: firstly, a higher strain rate creates a higher flow of stress which decelerates the dislocation annihilation and secondly, the higher strain rate also increases the obstruction of dislocation motion. The base alloy displays a continuous increase of tensile strength along with the increment of strain rate due to the continuous plastic deformation mechanism [33, 34]. But at a higher strain rate, the variation of strength in Si-added alloys is lower. It points out that the alloy's plastic deformation mechanism collapses when the strain rate increases. It is obvious that Si-rich intermetallics are responsible for this phenomenon considering the fact that the base alloys, which show a different trend than the Si-added alloys, have no Si-rich intermetallics. Beyond the eutectic composition, the alloy exhibits adverse effects because of the emergence of blocky primary Si which weakens the alloy matrix. During solidification, this type of primary Si creates pin hole like defects; as a result, there is lower bonding with the matrix resulting in a decrease in tensile strength. At a higher strain rate, a substantial amount of primary Si is formed in a disorganized manner; consequently, the strength goes down.

The average values of percentages of elongation measured with the different strain rates are graphically presented in Figure 4. As observed in the Figure for the % elongation vs strain rate, the elongation drops rapidly with the strain rate for all the alloys. It also demonstrates that the decreasing rate depends on the Si content of the alloys. A higher strain rate causes the flow stresses to be higher, initiating the early stage of deformation. It can be alleged that at increased strain rates, the material does not acquire enough time to flow and stop at grain boundaries; as a result, inferior elongations occur [35]. It can be stated that the experimental alloys considered at the peak ageing consists of the maximum numbers of fine precipitates. A higher Si-added alloy means a higher level of precipitates and higher obstruction of dislocation motion. So, the decline rate of % elongation is lower for higher Si-added alloys. The hypereutectic alloy shows severely lower values for their primary Si, as discussed earlier.

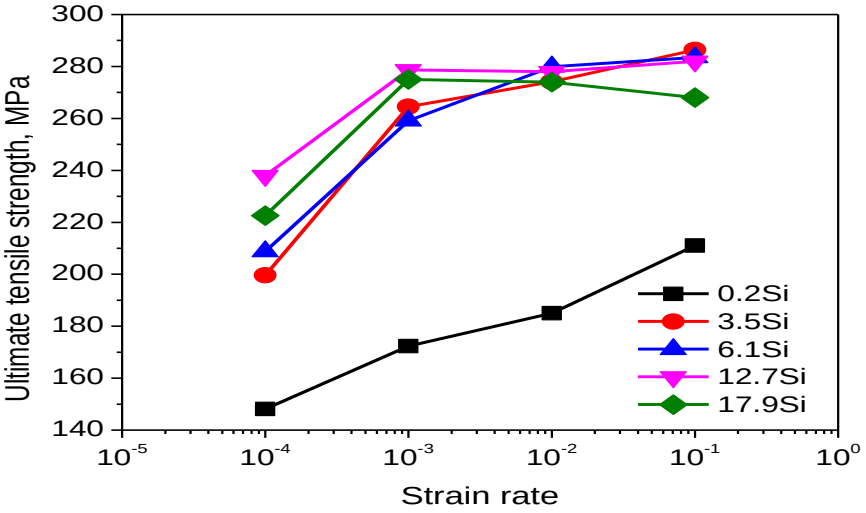

Figure 3. Ultimate tensile strength disparity with strain rate for different Si added alloys aged at 200 °C for 1h.

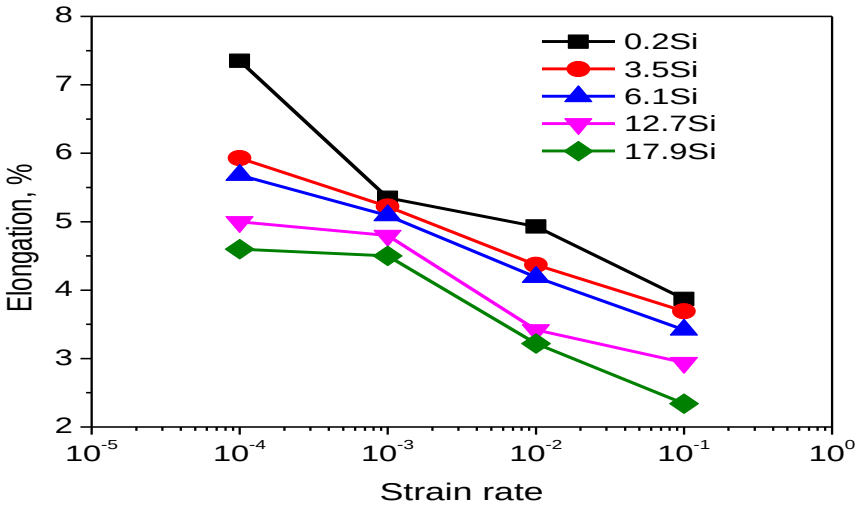

Figure 4. Percent elongation disparity with strain rate for different Si added alloys aged at 200 °C for 1h.

3.2 Impact energy

Based on the data tested from all the experimental alloys, the impact toughness properties at varied ageing treatment temperature can be observed from Figure 5. This Figure demonstrates that the impact strength decreases when the ageing temperature increases. This degradation of impact energy can be attributed to formation of the precipitation phases such as Al_2Cu, Al_2CuMg and Mg_2Si. These phases form as GP zones along with metastable phases leading to a major increase in the matrix strength at the cost of ductility. The fracture resistance decreases because of delicate precipitates, which act as the nucleation sites. The absorbed energy decreased to a minimum at peak aged conditions due to the maximum precipitation of intermetallic phases. The impact energy of the experimental alloys also varies with the variation of the Si content of the alloys. As the Si level is increased, the impact energy is relatively decreased. It is noticeable that higher Si creates a superior volume fraction of Si-rich precipitates [30, 36].

The strength increases considerably from peak-aged to over-aged situations owing to microstructural change through softening, precipitation coarsening as well as grain coarsening at the over-ageing temperature

[18]. At this over-aged condition, the alloys lose the brittleness as coarsened particles reduce the pinning effects. It may be noted that throughout the ageing treatment, the impact strength of the alloys fluctuates. It is already stated that heat treatment causes the precipitation formation of GP zones, β″, β′ and β, along with the Q″ phase [30]. The reduction of impact strength is associated with these precipitations, and the improvement is associated with the dissolution of these phases as the formation of a phase which occurs after the mandatory dissolution of the previous phase.

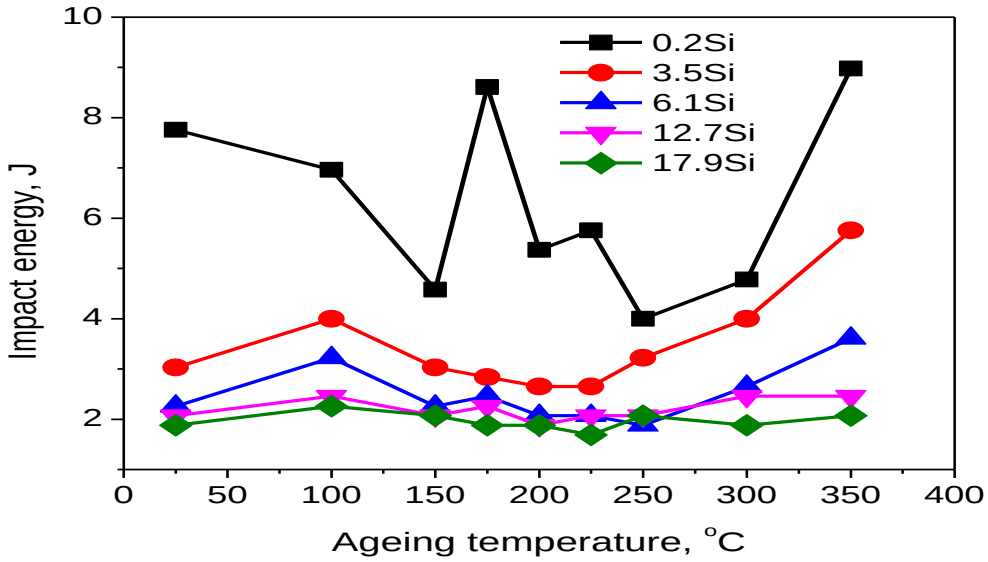

Figure 5. Fracture toughness evolution for different Si added alloys during isochronally ageing for 1h.

3.3 Optical microstructure

The optical microstructure of the different Si added automotive alloys aged at 200 °C for 1h are represented in Figure 6. Before ageing, the alloys are solutionized at 535 °C for 2h. The microstructures of the 0.2Si base alloy exhibits the α-Al phase with different intermetallic particles distribute in intragranular and grain boundary (Figure 6a) [37, 38]. As the amount of Si increases, eutectic phases begin to appear in the alloys as shown in Figure 6 (b) to (d). Additional eutectic silicon phases appear with the increase of silicon content, evident by the metallographic structure. Part of the silicon eutectic grains are clearly irregular and elongated, and the α-Al matrix phase has been replaced with a fragmented, dispersed silicon eutectic phase.

They are plate-like eutectic Si distributed at the grain boundary, making a coarse grain boundary [39]. Microstructural observation of the eutectic composition reveals dendrites of α-Al as the main constituent and elongated needle-like structures (flakes) of silicon are also observed. Beyond the eutectic composition, the 17.9Si added automotive alloy shows the star-shaped blocky primary Si on the background of an elongated needle-like eutectic structure (Figure 6e). It is conspicuous from the microstructures that there is low density of needle-like Si near the primary Si phase, which dictates a solute lean area in silicon near the primary Si and matrix interface [40]. More specifically the number of needle-like Si is less because some portion move to form the primary Si. Due to ageing, different types of precipitation arise within the matrix, but these fine precipitates cannot be exposed via this type of photography [41].

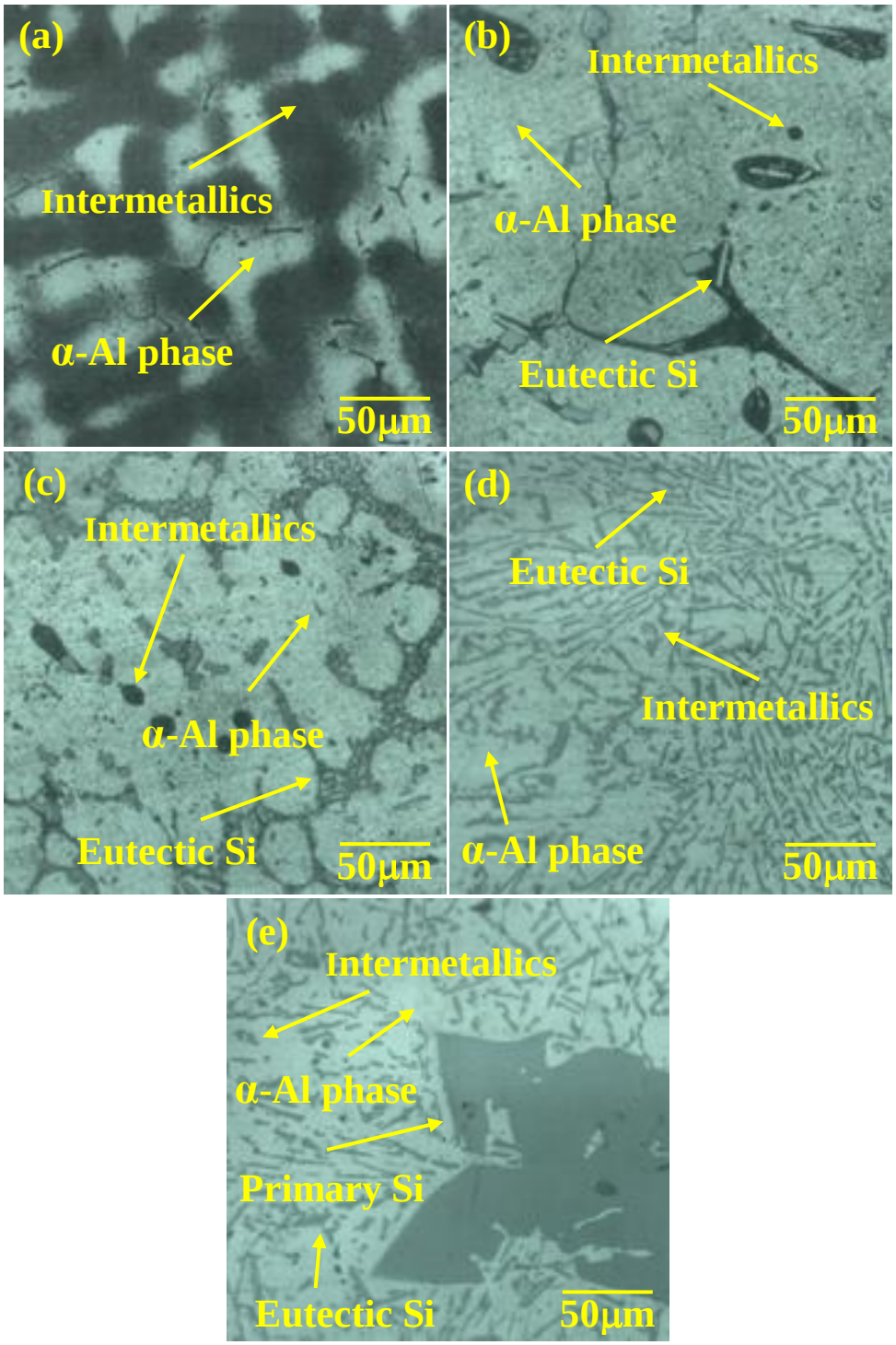

Figure 6. Optical micrographs of the automotive alloys a) 0.2Si, b) 3.5Si, c) 6.1Si, d) 12.7Si and e) 17.9Si under ageing treatment at 200 °C for 1h.

3.4 SEM fractography

Figure 7 shows the fracture morphology of the different Si content Al-based experimental alloys subjected to SEM analysis. The samples were solution treated in addition to being aged at 200ºC for 60 minutes and tensile tested at strain rate of 10^{-3}/s. The mode of fracture of the alloy's was observed to alter with the Si concentration of the alloys.

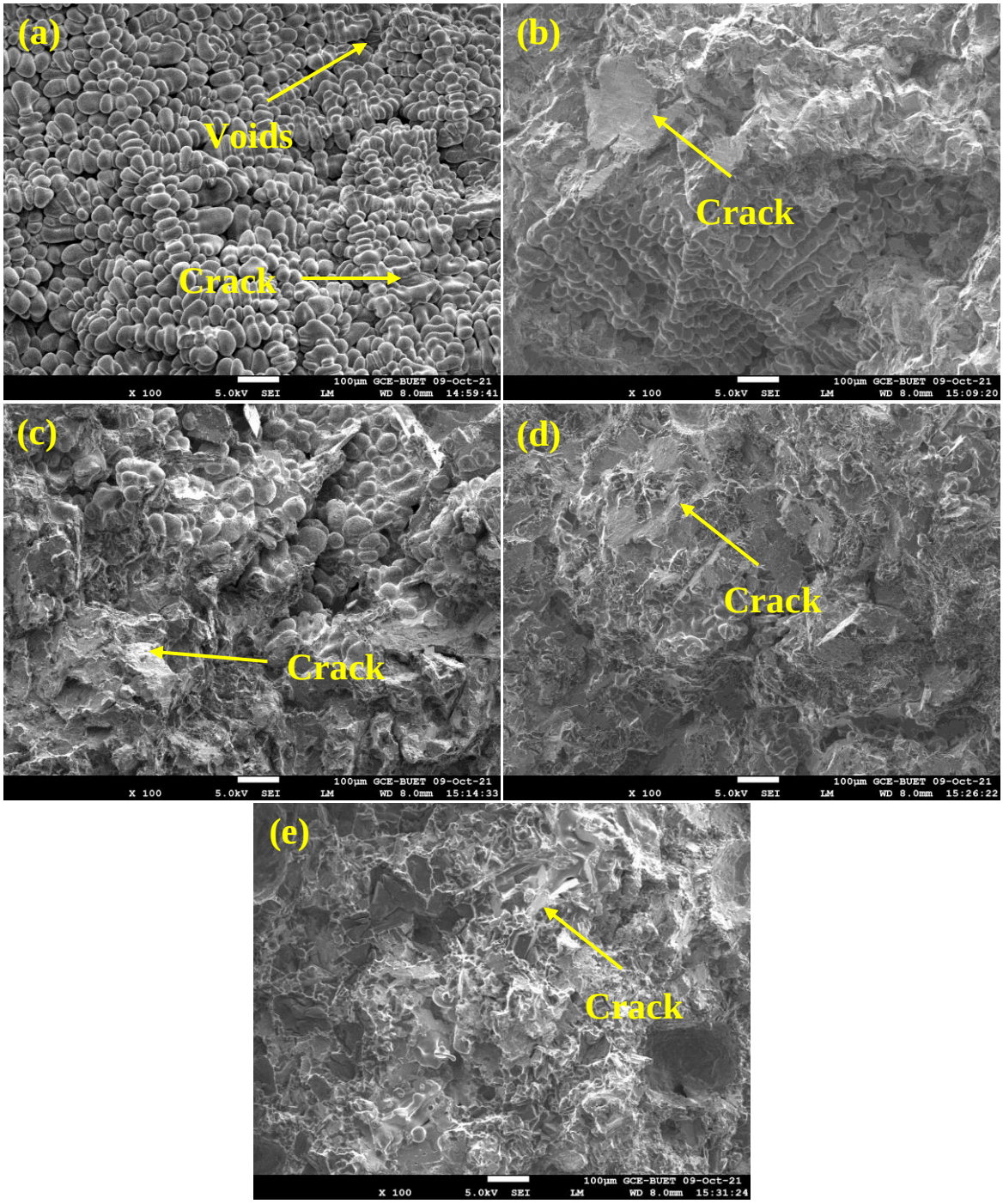

Figure 7. SEM fractograph of the different Si added automotive alloys a) 0.2Si, b) 3.5Si, c) 6.1Si, d) 12.7Si and e) 17.9Si under ageing treatment at 200 °C for 1h.

The fracture surface of the base alloy with 0.2Si exhibits a huge number of voids which is randomly distributed in the matrix of the alloy as shown in Figure 7(a). It is one of the most common fracture modes like intergranular fracture along with grain boundaries. Some simple morphology with a ductile α-phase fracture can be observed, which indicates a mixed fracture [42]. The Figure also demonstrates that the plane of the fracture depends on the orientation of the grain. With the increase of Si content, the alloys start to exhibit additional crack propagations triggered by the enormous cleavage of the plate-type shaped, brittle Si-rich intermetallics (Figure 7b). As Si content is increased, a significant amount of these intermetallics form in the alloys which extend the cracks (Figure 7c, d). The variety of crack direction also increases on fracture surfaces

with the increase of Si-rich intermetallics. There are many types of intermetallic phases observed in these types of alloys as they contain various alloying elements in different amounts; although plate-type shapes, intermetallics are the most damaging to mechanical properties [43, 44]. Beyond the eutectic composition, 17.9Si added alloy displays more cracks along with the void obtained by the massive cleavage and excess primary Si of eutectic composition (Figure 7e). Additional dimples are observed on the fracture surface because of the presence of higher Si-rich intermetallics in the higher Si-added alloy.

4 Conclusion

In this article, the following cases have been observed after an extensive investigation of the mechanical properties for the different level of Si doped Al-based automotive alloys under the ageing treatment.

- Two ageing peaks of Mg_2Si along with the Al_2Cu intermetallics through the GP zones and metastable phases are responsible for strengthening effects. The addition of Si accelerated the strength for the higher Si-rich intermetallice. Percentages of elongation and impact energy decrease as the outset of GP zones, β″, β′, β precipitate plus Q phases and increases significantly since precipitates and grain coarsening of the alloys, when aged at superior temperature. Higher Si-added alloy means a higher level of precipitates and the higher the obstruction of dislocation motion. So, the rate of % elongation is lower for higher Si-added alloys.
- The addition of Si showed earlier ageing peaks with different intensities. Si to become evident a solute diffusion enhancer, by binding itself to a vacancy and greater Si absorption in the α-Al matrix results in a better acceleration of solute diffusion kinetics.
- Tensile strength is affected by the strain rate and it is in a very small range when the Si is added in to the alloy. One is higher strain rate creates higher flow stress since decelerate the dislocation annihilation and other one it increases the obstruction of dislocation motion. Beyond the eutectic composition the alloy displays the negative effects due to presence of blocky primary Si as weaken the alloy matrix.
- The microstructures of the alloys reveal that the surface possesses the α-Al phase with different intermetallic particles distribute in intragranular along with grain boundary and Si eutectic phase a niddle-like come into view in addition the grain boundary coarsen when Si is added. Hypereutectic composition exhibited star-shaped blocky primary Si along with elongated needle-like eutectic structure.
- The fracture analysis with SEM micrographs demonstrates that in the base alloy, huge number of voids is consistently distributed in the matrix. Higher Si levels up to eutectic composition indicates additional spread of crack by the superior cleavage of the brittle Si-rich intermetallics. The hypereutectic alloy displays more cracks along with void obtained by the massive cleavage and excess primary Si of eutectic composition.

Acknowledgements

The corresponding author would like to thank Prof. Selina Nargis, the university's Treasurer and Director Administration, for her invaluable assistance and encouragement in fostering research activities there. Her initiatives to promote partnerships with other institutions have also been laudable.

References

[1] J. R. Davis, “Light Metals and Alloys,” Alloying: Understanding the Basics, 1st edition, ASM International, Ohio, USA, 2001.

[2] G. Mathers, “The Welding of Aluminium and its Alloys,” 1st edition, Woodhead Publishing, Sawston, Cambridge, UK, 2002.

[3] M. N. E. Efzan, H. J. Kong and C. K. Kok, “Review: Effect of Alloying Element on Al-Si Alloys, Advanced Materials Research, vol. 845, pp. 355-359, 2013, https://doi.org/10.4028/www.scientific.net/AMR.845.355.

[4] I. J. Polmear, Light Alloys-Metallurgy of the Light Metals, 3rd edition, Arnold, UK, 1995.

[5] H. S. Abdo, A. H. Seikh, J. A. Mohammed and M. S. Soliman, “Alloying Elements Effects on Electrical Conductivity and Mechanical Properties of Newly Fabricated Al Based Alloys Produced by Conventional Casting Process,” Materials, vol. 14, no. 14, pp. 1-10, 2021, https://doi.org/10.3390/ma14143971.

[6] J. C. Cisneros, R. P. Bustamante and R. M. Sanchez, "Al-Si-Cu Alloy Enhanced to High-Temperature Application by Nickel Addition," Revista Mexicana de Física, vol. 68, no. 3 pp. 1-7, 2022, https://doi.org/10.31349/RevMexFis.68.031004.

[7] M. S. Kaiser, M. R. Basher and A. S. W. Kurny, "Effect of Scandium on Microstructure and Mechanical Properties of Cast Al-Si-Mg Alloy," Journal of Materials Engineering and Performance, vol. 21, no. 7, pp. 1504-1508, 2012, https://doi.org/10.1007/s11665-011-0057-3.

[8] S. I. Park, S. Z. Han, S. K. Choi and H. M. Lee, "Phase Equilibria of Al3(Ti, V, Zr) Intermetallic System," Scripta mater, vol. 34, no. 11, pp. 1697-1704, 1996, https://doi.org/10.1016/1359-6462(96)00049-8

[9] G. Camicia and G. Timelli, "Grain Refinement of Gravity Die Cast Secondary AlSi7Cu3Mg Alloys for Automotive Cylinder Heads," Transactions of Nonferrous Metals Society of China, vol. 26, no. 5, pp. 1211-1221, 2016, https://doi.org/10.1016/S1003-6326(16)64222-X.

[10] S. K. Shaha, F. Czerwinski, D. L. Chen and W. Kasprzak, "Dislocation Slip Distance During Compression of Al–Si–Cu–Mg Alloy with Additions of Ti–Zr–V," Materials Science and Technology, vol. 31, no. 1, pp. 63-72, 2015, https://doi.org/10.1179/1743284714Y.0000000606.

[11] M. S. Kaiser, "Efffect of Solution Treatment on the Age Hardening Behaviour of Al-12Si-1Mg-1Cu Piston Alloy with Trace Zr Addition," Journal of Casting and Materials Engineering, vol. 2, no. 2, pp. 30-37, 2018, https://doi.org/10.7494/jcme.2018.2.2.30.

[12] M. A. Nur, A. A. Khan, S. D. Sharma and M. S. Kaiser, "Electrochemical Corrosion Performance of Si Doped Al-Based Automotive Alloy in 0.1 M NaCl Solution" Journal of Electrochemical Science and Engineering, vol. 12, no. 3, pp. 565-576, 2022, https://doi.org/10.5599/jese.1373.

[13] W. D. Zhang, J. Yang, J. Z. Dang, Y. Liu and H. Xu, "Effects of Si, Cu and Mg on the High-Temperature Mechanical Properties of Al-Si-Cu-Mg Alloy," Advanced Materials Research, vol. 652–654, pp. 1030-1034, 2013, https://doi.org/10.4028/www.scientific.net/amr.652-654.1030.

[14] J. R. Davis, "ASM Specially Handbook, Aluminum and Aluminum alloys," ASM International Publications, Materials Parks, OH, USA, 1993.

[15] Q. Chen, W. Zhao, J. Jiang, M. Huang, M. Li, Y. Wang, C. Ding and D. Zou, "Effect of T6 heat treatment on microstructure and mechanical properties of large-weight aluminum alloy flywheel housing parts formed by local-loading squeeze casting," Journal of Materials Research and Technology, vol. 24, pp. 1612-1625, 2023. https://doi.org/10.1016/j.jmrt.2023.03.084.

[16] S. Toschi, "Optimization of A354 Al-Si-Cu-Mg Alloy Heat Treatment: Effect on Microstructure, Hardness, and Tensile Properties of Peak Aged and Overaged Alloy," Metals, vol. 8(11), no. 961, pp. 1-16. 2018, https://doi.org/10.3390/met8110961.

[17] H. Mao, X. Bai, F. Song, Y. Song, Z. Jia, H. Xu and Y. Wang, "Effect of Cd on Mechanical Properties of Al-Si-Cu-Mg Alloys under Different Multi-Stage Solution Heat Treatment," Materials (Basel), vol. 15, no. 15, pp. 1-14, 2022, https://doi.org/10.3390/ma15155101.

[18] M. S. Kaiser, "Solution Treatment Effect on Tensile, Impact and Fracture Behaviour of Trace Zr Added Al-12Si-1Mg-1Cu Piston Alloy," Journal of the Institution of Engineers, India, Series D, vol. 99, no. 1, pp. 109-114, 2018, https://doi.org/10.1007/s40033-017-0140-5.

[19] S. S. Ahn, S.Pathan, J. M. Koo, C. H. Baeg, C. U. Jeong, H. T. Son, Y. H. Kim, K. H. Lee and S. J. Hong, "Enhancement of the Mechanical Properties in Al–Si–Cu–Fe–Mg Alloys with Various Processing Parameters," Materials (Basel). Vol. 11, no. 11, pp. 1-12, 2018, https://doi.org/10.3390/ma11112150.

[20] M. S. Kaiser, S. Sabbir, M. S. Kabir, M. R. Soummo and M. A. Nur, "Study of Mechanical and Wear Behaviour of Hyper-Eutectic Al-Si Automotive Alloy through Fe, Ni and Cr Addition," Materials Research, vol. 21, no. 4, pp. 1-9, 2018, https://doi.org/10.1590/1980-5373-MR-2017-1096. .

[21] S. Liu, K. Li, J. Lu, G. Sha, J. Wang, M. Yang, G. Ji, M. Song, J. Wang and Y. Du, "On the atomic model of Guinier-Preston zones in Al-Mg-Si-Cu alloys," Journal of Alloys and Compounds, vol. 745, pp. 644-650, 2018. https://doi.org/10.1016/j.jallcom.2018.01.304.

[22] R. X. Li, R. D. Li, Y. H. Zhao, L. He, C. X. Li, R. R. Guan and Z. Q Hu, "Age-Hardening Behavior of Cast Al-Si Base Alloy," Materials Letters, vol. 58, no. 15, pp. 2096-2101, 2004, https://doi.org/10.1016/j.matlet.2003.12.027.

[23] M. Zamani, S. Toschi, A. Morri, L. Ceschini and S. Seifeddine, "Optimisation of Heat Treatment of Al–Cu–(Mg–Ag) Cast Alloys," Journal of Thermal Analysis and Calorimetry, vol. 139, no. 6, pp. 3427-3440, 2020, https://doi.org/10.1007/s10973-019-08702-x.

[24] B. Zhang, L. Zhang, Z. Wang and A Gao, "Achievement of High Strength and Ductility in Al–Si–Cu–Mg Alloys by Intermediate Phase Optimization in As-Cast and Heat Treatment Conditions," Materials (Basel), vol. 13, no. 3, pp. 1-14, 2020, https://doi.org/10.3390/ma13030647.

[25] P. A. B. Machado, J. M. V. Quaresma, A. Garcia and C. A. Santos, "Investigation on Machinability in Turning of As-Cast and T6 Heat-Treated Al-(3, 7, 12%) Si-0.6%Mg Alloys," Journal of Manufacturing Processes, vol 75, no. 1, pp. 514-526, 2022, https://doi.org/10.1016/j.jmapro.2022.01.028.

[26] H. Choi and X. Li, "Refinement of primary Si and modification of eutectic Si for enhanced ductility of hypereutectic Al-20Si-4.5Cu alloy with addition of Al_2O_3 nanoparticles," Journal of Materials Science, vol. 47, no. 7, pp. 3096-3102, 2012, https://doi.org/10.1007/s10853-011-6143-y.

[27] L. Liu, J. H. Chen, S. B, Wang, C. H. Liu, S. S. Wang and C. L. Wu, "The effect of Si on precipitation in Al–Cu–Mg alloy with a high Cu/Mg ratio," Materials Science and Engineering: A, vol. 606, pp. 187-195, 2014, https://doi.org/10.1016/j.msea.2014.03.079.

[28] N. Q. Vo, D. C. Dunand and D. N. Seidman, "Role of silicon in the precipitation kinetics of dilute Al-Sc-Er-Zr alloys," Materials Science & Engineering A, vol. 677, pp. 485-495, 2016, https://doi.org/10.1016/j.msea.2016.09.065.

[29] A. M. A. Mohamed, E. Samuel, Y. Zedan, A. M. Samuel, H. W. Doty and F. Samuel, "Intermetallics formation during solidification of Al-Si-Cu-Mg cast alloys, Materials (Basel), vol. 15, no. 4, pp. 1-24, 2022, https://doi.org/10.3390/ma15041335.

[30] F. Czerwinski, "Heat Treatment," IntechOpen, Rijeka, Croatia, 2012.

[31] R. Guan, Y. Shen and Z. Zhao, "A High-Strength, Ductile Al-0.35Sc-0.2Zr Alloy with Good Electrical Conductivity Strengthened by Coherent Nanosized-Precipitates," Journal of Materials Science & Technology, vol.33, no. 3, pp. 215-223, 2017, https://doi.org/10.1016/j.jmst.2017.01.017.

[32] Y. Wang, H. Liao, Y. Wu and J. Yang, "Effect of Si content on microstructure and mechanical properties of Al–Si–Mg alloys," Materials and Design, vol. 53, pp. 634-638, 2014, https://doi.org/10.1016/j.matdes.2013.07.067.

[33] R. Bobbili, V. Madhu and A. K. Gogia, "Tensile Behaviour of Aluminium 7017 Alloy at Various Temperatures and Strain Rates," Journal of Materials Research and Technology, vol. 5, no. 2, pp. 190-197, 2016, https://doi.org/10.1016/j.jmrt.2015.12.002.

[34] L. Wang, Y. Liu, X. Song, J. Jin and B. Zhang, "Tensile Deformation Behavior of a Nickel-base Superalloy under Dynamic Loads," 13th International Conference on Fracture, Beijing, China, 16-21 June 2013.

[35] H. Solouki, E. Borhani and M. T. Nezhad, "The effect of temperature and strain rate on elongation to failure in nanostructured Al-0.2wt% Zr alloy fabricated by ARB process," Journal of Ultrafine Grained and Nanostructured Materials, vol.48, no.2, pp.125-132, 2015, https://doi.org/10.7508/jufgnsm.2015.02.007.

[36] M. S. Kaiser, S. Datta, A. Roychowdhury and M. K. Banerjee, "Effect of Scandium Additions on the Tensile Properties of Cast Al-6Mg Alloys," Journal of Materials Engineering and Performance," vol. 17, no. 6, pp. 902-907, 2008, https://doi.org/10.1007/s11665-008-9242-4.

[37] K. Liu, X. Cao and X. G. Chen, "Effect of Mn, Si, and Cooling Rate on the Formation of Iron-Rich Intermetallics in 206 Al-Cu Cast Alloys," Metallurgical and Materials Transactions B, vol. 43, no. 5, pp. 1231-1240, 2012, https://doi.org/10.1007/s11663-012-9694-7.

[38] T. T. Alshammari, H. F. Alharbi , M. S. Soliman and M. F. Ijaz, "Effects of Mg Content on the Microstructural and Mechanical Properties of Al-4Cu-xMg-0.3Ag Alloys," Crystals, vol.10, no. 895, pp. 1-13, 2020, https://doi.org/10.3390/cryst10100895.

[39] S. P. Nikanorov, M. P. Volkov, V. N. Gurin, Y.. A. Burenkov, L. I. Derkachenko, B. K. Kardashev, L. L. Regel and W. R. Wilcox, "Structural and mechanical properties of Al–Si alloys obtained by fast cooling of a levitated melt," Materials Science and Engineering: A, vol. 390, no. 1-2, pp. 63-69, 2005, https://doi.org/10.1016/j.msea.2004.07.037.

[40] M. R. Alawandi, S. S. Khaji and D. M. Goudar, "Microstructure and Mechanical Properties of Spray Formed and Hot-Pressed Hypereutectic AlSi Alloy," Research & Development in Material Science, vol. 11, no. 1, pp. 1134-1140, 2019. https://doi.org/10.31031/RDMS.2019.11.000755.

[41] G. G. Sirata, K Wacławiak and M. Dyzia, "Mechanical and Microstructural Characterization of Aluminium Alloy, EN AC-Al Si12CuNiMg," Archives of Foundry Engineering, vol. 22, no. 3, pp. 34-40, 2022. https://doi.org/10.24425/afe.2022.140234.

[42] S. Lynch, "A Review of Underlying Reasons for Intergranular Cracking for a Variety of Failure Modes and Materials and Examples of Case Histories," Engineering Failure Analysis, vol. 100, pp. 329-350, 2019, https://doi.org/10.1016/j.engfailanal.2019.02.027.

[43] Y. Meng, H. Zhang, X. Li, X. Zhou, H. Mo, L. Wang and J. Fan, "Tensile Fracture Behavior of 2A14 Aluminum Alloy Produced by Extrusion Process," Metals, vol. 12, no. 184, pp. 1-13, 2022, https://doi.org/10.3390/met12020184.

[44] D. A. Lados, D. Apelian and J. F. Major, "Fatigue Crack Growth Mechanisms At the Microstructure Scale in Al-Si-Mg Cast Alloys: Mechanisms in Regions II and III.," Metallurgical and Materials Transactions A., vol. 37A, no. 8, pp. 2405-2418, 2006, https://doi.org/10.1007/BF02586215.